THE JOURNAL OF PHYSICAL CHEMISTRY C

Article

pubs.acs.org/JPCC

Semiclassical Plexcitonics: Simple Approach for Designing Plexcitonic Nanostructures

Daniel E. Gómez,*[,†,‡] Harald Giessen,[§] and Timothy J. Davis[†,‡]

[†]CSIRO, Materials Science and Engineering, Private Bag 33, Clayton, Victoria 3168, Australia

[‡]Melbourne Centre for Nanofabrication, Australian National Fabrication Facility, Clayton, Victoria 3168, Australia

[§]4th Physics Institute, University of Stuttgart, Pfaffenwaldring 57, 70569 Stuttgart, Germany

Supporting Information

ABSTRACT: We present a classical description of the interaction between localized surface plasmon resonances and excitons which can occur in molecular or solid state systems. Our approach consists of adopting a semianalytical description of the surface plasmon resonances in metal nanoparticles and a semiclassical description of the electronic transitions related to the excitonic material. We consider three plasmon-exciton coupling configurations, namely a (or a set of) metal nanoparticle(s) uniformly coated with an excitonic material, a set of metal nanoparticles placed in the vicinity of a sub-wavelength-sized "patch" containing the active material, and the limiting case of a single point dipole coupled to a metal nanoparticle. Our key result is the derivation of the conditions required to achieve strong plasmon−exciton coupling as evidenced by polaritonic splitting. We apply our results to describe recent experimental studies on these hybrid systems. Our study provides a simple, yet rigorous prescription to both analyze and design systems that exhibit strong light−matter interactions as mediated by localized surface plasmon resonances (i.e., particle plasmons).

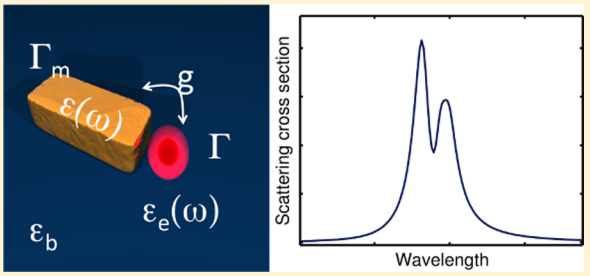

Surface plasmon resonances in metallic nanoparticles have attracted a significant amount of research due to the sub-wavelength confinement of light that is possible with these collective excitations. When a surface plasmon field interacts with electronic excitations such as excitons, two interaction regimes are possible, one of which (the strong coupling regime) results in the formation of plasmon−exciton hybrid states or *plexcitons*.[1] These hybrid states are characterized by avoided crossings in dispersion diagrams of the coupled system that are manifest in scattering or reflectivity spectra as spectral doublets. To date, plexcitons have been experimentally achieved in many configurations,[1−31] including thin metal films with thin excitonic layers,[2,9,12,18,19,28] monolayer coatings on nanoparticles,[1,16,23,24] and homogeneous thin films covering nanoparticles.[29]

Plexcitons are Bosonic quasi-particles half exciton, half plasmons which possess the lightest to-date reported effective masses, a feat that could make possible the observation of Bose−Einstein condensation at room temperature.[27] Plexcitons are also promising candidates for demonstrating polariton lasing at the nanoscale with highly reduced thresholds as compared to conventional lasers, and unlike conventional polariton devices that have required the use of micron-sized optical cavities,[32,33] plexciton states can readily occur in single metal nanoparticles which are inherently sub-wavelength sized.

In order to create structures that support plexciton states, the obvious requirement is that these structures should be composed of a surface plasmon supporting element that interacts strongly with an excitonic material. Aside from this simple requirement, here we investigate what are the specific material requirements needed when the plasmonic structures consist of single or coupled metallic nanoparticles which interact with an excitonic material in the form of (a) a uniform coating around the plasmonic elements, (b) a nanostructured "patch", and (c) a single emitter positioned in the near-field of the plasmonic nanostructures, as depicted in the diagram of Figure 1. To this end, we develop a semianalytical model based on the Electrostatic Eigenmode Method (EEM)[34] that is employed for describing the surface plasmon resonance in metal nanoparticles and a semiclassical description of the electronic transitions related to the excitonic material. Our results provide a guide that is useful in designing plexcitonic systems.

In the EEM one solves Maxwell's equations for metal nanoparticles assuming that these are much smaller than the wavelength of light. Within this approximation, the optical properties of particles are described in terms of eigenmodes, which are self-sustained surface charge oscillations that occur at the surface of the particles.[35] According to this approximation, the optical properties of coupled nanoparticles can be thought as originating from linear superpositions of the eigenmodes of the noninteracting nanoparticles.[36] This permits a description

Received: June 27, 2014
Revised: September 14, 2014
Published: September 17, 2014

   dx.doi.org/10.1021/jp506402m | J. Phys. Chem. C 2014, 118, 23963−23969

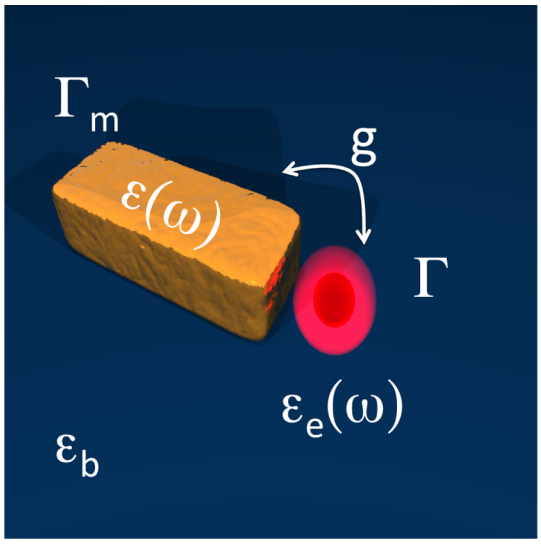

Figure 1. Configuration of plasmon−exciton coupling. g is the coupling strength, Γ_m is a rate representing the losses in the plasmon mode m and Γ the losses in the excitonic system. $\varepsilon(\omega)$ is the permittivity of the metal, $\varepsilon_e(\omega)$ the permittivity of the excitonic system, and ε_b that of the surrounding dielectric medium. Here, we consider the cases where the nanoparticles are homogeneously coated with the "excitonic" material or when they interact with "patches" of emitters and single emitters, as depicted in this figure.

of the optical properties of complex arrays of nanoparticles by using group theoretical analysis.[37] In spite of its approximate nature, the EEM can explain several experimental observations, including the effect of the substrate on the resonances of metal nanoparticles,[38] the optical modes of nanoparticle chains,[39,40] the optical response of 3D nanostructures,[41] the generation of optical chirality,[42,43] and the optical excitation of collective dark modes.[44]

According to the EEM, optical excitation of nanoparticles results in oscillating charge densities σ at the surface of metal nanoparticles which can be decomposed into superpositions of the normal modes of the nanoparticles σ_{pm} where each mode m of particle p is associated with an eigenvalue γ_{pm} that dictates the resonance wavelength (a real-valued quantity) of the surface plasmon mode through the following relationship:

$$\mathrm{Re}\{(\gamma_{pm} - 1)\varepsilon(\omega_{pm}) + (1 + \gamma_{pm})\varepsilon_b\} = 0 \tag{1}$$

with $\varepsilon(\omega)$ the (complex) metal permittivity and ε_b the permittivity of the surrounding medium. For the case of an ellipsoid, γ_{pm} can be related to the depolarization factors.[38] This very simple relationship can be used to describe the resonances of metal nanoparticles when these interact with uniform and spatially homogeneous media containing an exciton transition.

In the experiments of Schlather et al.,[29] Au nanodisks were embedded in a PVA matrix doped with J-aggregates of a cyanine dye, and under certain experimental conditions, they observed doublets in the measured scattering spectra of the nanoparticles, a characteristic of the formation of plexciton states in this system.

Within the EEM, the observation of spectral doublets in a configuration consisting of metal nanoparticles in a uniform and infinite medium containing J-aggregates (the excitonic material) can be fully accounted for by using eq 1. To this end, the permittivity ε_e of the excitonic material is described by

$$\varepsilon_e(\omega) = \varepsilon_\infty - \frac{f\omega_o^2}{\omega^2 - \omega_o^2 + i\Gamma\omega} \tag{2}$$

where ε_∞ is a parameter describing the permittivity at wavelengths above the resonance frequency ω_o. Γ is the line width of the transition, f is its reduced oscillator strength, and the permittivity of the metal is described by a Drude model: $\varepsilon(\omega) = \varepsilon_\infty^D - \omega_P^2/(\omega^2 + i\omega\Gamma_m)$.

Using eq 1 with the Drude model for $\varepsilon(\omega)$ near a plasmon resonance ω_m [as done in ref 35; see Supporting Information section, eq S3], eq 2 is combined for ε_e, assuming that $\omega \approx \omega_o$, which leads to

$$\varepsilon_\infty^D - \frac{\omega_P^2}{\omega_m^2} + \frac{2\omega_P^2}{\omega_m^3}(\omega - \omega_m + i\Gamma_m/2) = \left(\frac{1 + \gamma_{pm}}{1 - \gamma_{pm}}\right)\left(\varepsilon_\infty - \frac{f\omega_o}{2(\omega - \omega_o + i\Gamma/2)}\right) \tag{3}$$

where the value of the plasmon resonance ω_m is obtained as [see section S2, eq S5]:

$$\varepsilon(\omega_m) = \left(\frac{1 + \gamma_{pm}}{1 - \gamma_{pm}}\right)\varepsilon_\infty \approx \varepsilon_\infty^D - \frac{\omega_P^2}{\omega_m^2} \tag{4}$$

To simplify notation, we introduce the following complex frequencies $\tilde{\omega}_o = \omega_o - i\Gamma/2$ and $\tilde{\omega}_m = \omega_m - i\Gamma_m/2$. It is straightforward to show that the equation for the resonance frequency of the metal particles in the excitonic medium is

$$(\omega - \tilde{\omega}_o)(\omega - \tilde{\omega}_m) = \frac{1 + \gamma_{pm}}{\gamma_{pm} - 1}\frac{f\omega_o\omega_m^3}{4\omega_P^2} \tag{5}$$

which leads to a quadratic equation whose two roots $\omega_\pm$ are given by

$$\omega_\pm = \frac{\omega_o + \omega_m}{2} + \frac{i(\Gamma + \Gamma_m)}{4} \pm \sqrt{g^2 + \left(\frac{\tilde{\omega}_m - \tilde{\omega}_o}{2}\right)^2} \tag{6}$$

where we have defined the plasmon−exciton coupling constant as

$$g_{pm}^2 \equiv \left(\frac{1 + \gamma_{pm}}{\gamma_{pm} - 1}\right)\frac{\omega_m^3}{2\omega_P^2} \times \frac{f\omega_o}{2} \tag{7}$$

According to eq 6, the condition required for observing two distinct (real valued) resonances when $\omega_o = \omega_m$ is $g_{pm}^2 > (\Gamma_m - \Gamma)^2/16$, which is the "strong coupling condition", a result consistent with studies of strong coupling in microcavities.[45−47] The splitting in this case is given by $2[g_{pm}^2 - (\Gamma_m - \Gamma)^2/16]^{1/2}$, which in order to result in clearly resolvable spectral doublets must additionally exceed the value of the average line widths $(\Gamma + \Gamma_m)/4$.

The most significant aspect of this result is that this strong coupling condition has no dependence on the magnitude of the electric near-field around the nanoparticle. More explicitly, resonance splitting in these plasmon−exciton systems does not depend on the presence of hot spots in the metallic nanostructures when these are homogeneously coated with the excitonic material. Instead, in this case the coupling strength as written in eq 7 depends on the material properties of the excitonic material through f and ω_o and those of the metal

dx.doi.org/10.1021/jp506402m | J. Phys. Chem. C 2014, 118, 23963−23969

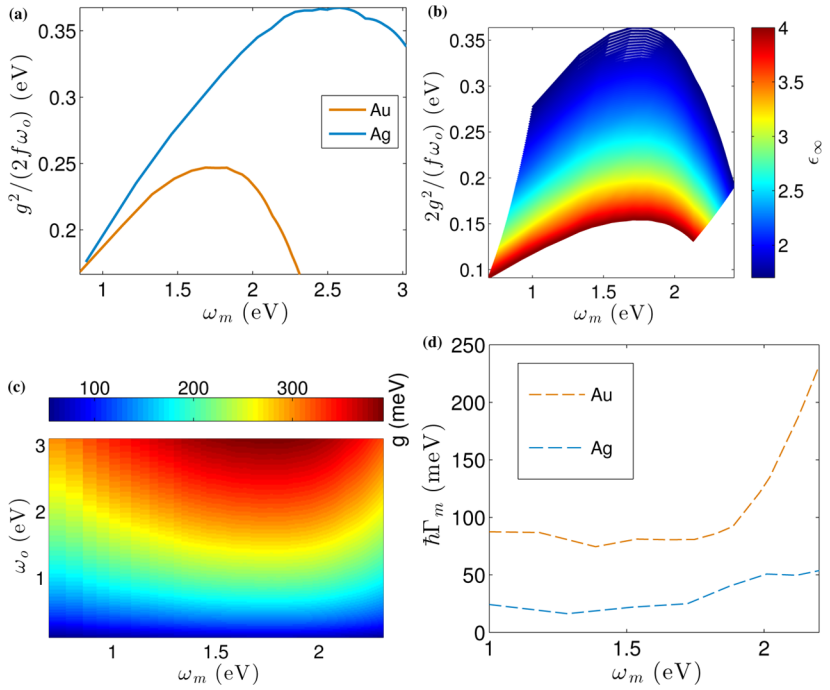

Figure 2. (a) Plasmon−exciton coupling constant g^2 [eq 7] vs particle plasmon resonance frequency ω_m for $\varepsilon_\infty = 2.5$. In these calculations, $\omega_P = 9.04$ eV for Ag and $\omega_P = 8.62$ eV for Au. (b) Evolution of $2g^2/(f\omega_o)$ vs the localized surface plasmon resonance ω_m with the value of ε_∞ for Au. (c) g calculated vs ω_m and ω_o for $\varepsilon_\infty = 2.5$ and $f = 0.4$. (d) Intrinsic line width of a localized surface plasmon resonance plotted vs particle plasmon resonance frequency ω_m for $\varepsilon_\infty = 2.5$. for Au and Ag.

through the value of the plasma frequency ω_P, the eigenvalue γ_{pm} ($\gamma_{pm} > 1$) which is a shape-dependent parameter, and the localized surface plasmon resonance ω_m, which is an implicit function both of the ε_∞ of the excitonic medium and γ_{pm} as of eq 4 (see also, Figure S1). Clearly, when $g_{pm}^2 < (\Gamma_m - \Gamma)^2/16$, the plasmon resonance is only weakly perturbed and one would expect to observe a red shift in the position of the plasmon resonance with an increase in its line width. Equation 7 quantifies the plasmon−exciton coupling strength for a plasmon mode m characterized by a surface charge distribution σ_{pm} which, through its associated dipole moment, dictates how the mode interacts with light.[36]

Let us now examine in more detail the dependence of g_{pm} on the material properties of the metal. In Figure 2a, we show how g_{pm}^2 (as normalized to the properties of the excitonic material, i.e., divided by $f\omega_o/2$) changes as a function of localized surface plasmon frequency (energy) for Au and Ag in a medium with $\varepsilon_\infty = 2.25$. In this case, the eigenvalue γ_{pm} is allowed to vary, and according to eq 4, there is a one-to-one mapping between the eigenvalue and the localized surface plasmon resonance frequency (ω_m increases with increasing γ_{pm} as shown in Figure S1 of the Supporting Information). This situation therefore corresponds to the case of having a fixed excitonic medium and metal nanoparticles of different shapes or different resonance frequencies. Figure 2a shows clearly that Ag exhibits the strongest coupling strength across the entire spectrum. Additionally, g_{pm}^2 seems to peak for either metal at a particular frequency: 1.83 eV for Au and 2.58 eV for Ag. g^2 decreases strongly when ω_m approaches either the interband transitions of the metals or the near-infrared. Figure 2b shows that the (normalized) value of g_{pm}^2 also decreases with increasing the value of ε_∞ of eq 2, indicating that strong coupling can be more easily observed for excitonic materials with a low background permittivity, which is typically the case for organic semiconductors. At the peak value shown in Figure 2a, one would therefore expect to obtain the strongest coupling which will manifest as a large spectral splitting. Figure 2c shows how the coupling constant g_{pm} varies with the localized surface plasmon frequency (energy) ω_m for Au and the resonance frequency (energy) ω_o of an excitonic medium described by eq 2 with $\varepsilon_\infty = 2.25$ and $f = 0.4$ typical values for thin polymer films doped with J-aggregates.[2,29] Similar to the case shown in Figure 2a, the highest values for g_{pm} are obtained when the localized plasmon resonances ω_m are in the spectral region between 1.5 and 2 eV, but these high values also occur when the resonance frequency of the excitonic medium ω_o is slightly detuned (blueshifted) from the plasmon resonance. This is partly due to the fact that eq 7 for g_{pm} has different dependencies on ω_o ($g_{pm} \propto \sqrt{\omega_o}$) and ω_m ($g_{pm} \propto (\omega_m^3)^{1/2}$).

The predictions of Figure 2b however do not completely specify the conditions for strong coupling, since as previously stated, in order to achieve this regime, g_{pm} has to exceed the losses in the coupled system.

For Au nanoparticles, the losses can be decomposed into three contributions:[48] intrinsic bulk damping mechanisms, surface scattering, and radiative losses. The first mechanism is due to electron inelastic scattering by phonons, impurities, and defects and is generally a process described by the dielectric permittivity of the metal which contributes to the surface plasmon line width as indicated in Figure 2d. The contribution of surface scattering to the line width is given by[48,49] $\Gamma_s = A\nu_F/L_{\text{eff}}$, with A as a constant of the order of unity, ν_F the Fermi velocity, and L_{eff} the effective path length of the electrons. Radiative damping on the other hand is approximately given by[48,49] $\Gamma_r = 2\hbar\kappa V$, with κ as a phenomenological constant and V the volume of the nanoparticle. The net effect of the appearance of L_{eff} and V in these two expressions is that the contribution of these two damping mechanisms to the total

dx.doi.org/10.1021/jp506402m | J. Phys. Chem. C 2014, 118, 23963−23969

surface plasmon line width Γ_m depends on the geometry of the nanoparticles, setting thus the dashed lines shown in Figure 2c as the lower limits to the total surface plasmon mode line width.

Armed with a description of the plasmonic contribution to the coupling strength g and to the losses in the coupled systems, our attention is now focused on the excitonic materials and their material properties, as described by eq 2, which are required to achieve strong plasmon−exciton coupling. To this end, we proceed first by drawing an example from the literature and consider in Figure 3 the attainable coupling strengths g_{pm} for an excitonic medium described with eq 2, namely: DPDC (2,2′-dimethyl-8-phenyl-5,6,5′,6′-dibenzothiacarbocyanine chloride) J-aggregates,[29] for which $\varepsilon_\infty = 2.5$, $f = 0.4$, $\omega_o = 1.79$ eV, and $\hbar\Gamma = 52$ meV.

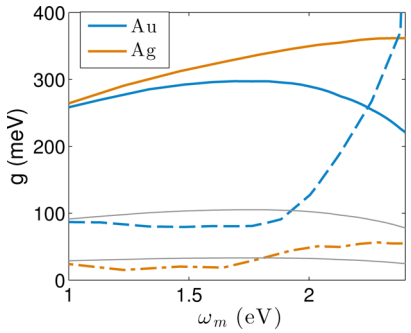

Figure 3. Plasmon−exciton coupling constant g_{pm} calculated for DPDC J-aggregates plotted vs localized plasmon resonance frequency ω_m for Au and Ag. Also shown (dotted and dashed lines) are the lower limits to the line width of the surface plasmon resonance. The gray lines correspond to the calculated coupling constant with the minimum values of f that would still result in strong coupling.

Figure 3 clearly shows that, for both Ag and Au nanoparticles uniformly coated with DPDC, g_{pm} is always larger than the average line widths $(\Gamma + \Gamma_m)/4$ (discontinuous lines in Figure 3) and thus the observation of a strong plasmon−exciton is very likely in this case, in agreement with the results of Schlather et al.[29] For the case presented by Schlather et al.,[29] our model predicts a splitting of 590 meV which is larger than the one experimentally measured (230−400 meV). Our estimate ignores radiative damping, the effect of which is to decrease this value. By artificially decreasing the value of f and evaluating eq 7 (only f and ω_o describe the J-aggregates in this equation), our simple model predicts that in order to realize strong coupling to localized surface plasmon resonances, the minimum value of the reduced oscillator strength required for Au in the 1.5 to 2 eV spectral region is $f \gtrsim 5 \times 10^{-2}$ and for Ag this is $f \gtrsim 5 \times 10^{-3}$ (see gray lines in Figure 3; in the Supporting Information, we give details on how these f values translate into absorption cross sections). One question that naturally arises: is it possible to improve the coupling by nanostructuring both the plasmonic and excitonic elements? We consider this in the following section.

A single dipole emitter/absorber can be modeled as a polarizable dielectric sphere with a complex dielectric function $\varepsilon_e(\omega)$ given by that of eq 2.

For a single or set of coupled metal nanoparticles proximal to this excitonic material, the surface plasmon excitations can be written as[36] $\sigma = \Sigma_m \tilde{a}_m \sigma_m$, where the index m indicates the surface plasmon mode (i.e., for a spherical particle, m can indicate modes such as the dipole-like, quadrupole-like mode, etc.). The coefficients $\tilde{a}_m$ are the excitation amplitudes for the coupled system, which according to the EEM can be written in terms of the "uncoupled" excitation amplitudes a_m of its constituents. a_m for a metallic nanoparticle is approximately given by[35] $a_m \approx f_m(\omega)\vec{p}_m \cdot \vec{E}$, where $f_m(\omega)$ is a frequency and shape dependent function describing the spectral properties of the plasmon resonance (more details in section S4), $\vec{p}_m$ is the dipole moment of the m-th surface plasmon mode, and $\vec{E}$ is the total electric field incident of the particle. For a single plasmon mode interacting with a single emitter, the total electric field that drives the localized surface plasmon mode consists of the applied field $\vec{E}_o$ plus the field originating from the single emitter: $\tilde{a}_s\vec{E}_s$. In this case, the excitation amplitude is modified to $\tilde{a}_m$ and is given by (more details in section S4)

$$\begin{aligned}\tilde{a}_m &= f_m(\omega)\vec{p}_m \cdot (\vec{E}_o + \tilde{a}_s\vec{E}_s) \\ &= a_m + f_m(\omega)\langle \vec{p}_m \cdot \vec{E}_s \rangle \tilde{a}_s = a_m + f_m(\omega) G_{ms}\tilde{a}_s\end{aligned} \tag{8}$$

Similarly, the excitation amplitude of the single emitter is also expressed as[50,51]

$$\begin{aligned}\tilde{a}_s &= f_s(\omega)\vec{p}_s \cdot (\vec{E}_o + \tilde{a}_m\vec{E}_m) \\ &= a_s + f_s(\omega)\langle \vec{p}_s \cdot \vec{E}_m \rangle \tilde{a}_m = a_s + f_s(\omega) G_{sm}\tilde{a}_m\end{aligned} \tag{9}$$

with $\vec{p}_s$ as the induced dipole moment on the dielectric sphere and G_{sm} as the sphere-to-metal coupling coefficient. It is worth noting here that both $\vec{E}_s$ and $\vec{E}_m$ are the electric fields produced by the eigen-modes of the dielectric sphere (a three-fold degenerate dipolar mode[50,51]) and the m-th surface plasmon eigenmode of the metallic nanoparticles, and that furthermore $\langle \cdots \rangle$ denotes a spatial average of these fields in either the metal nanoparticle or the dielectric sphere (more details in section D of the Supporting Information).

These two linear equations can be combined as follows:

$$\begin{aligned}\begin{pmatrix}\tilde{a}_m \\ \tilde{a}_s\end{pmatrix} &= \begin{pmatrix}1 & -f_m G_{ms} \\ -f_s G_{sm} & 1\end{pmatrix}^{-1}\begin{pmatrix}a_m \\ a_s\end{pmatrix} \\ &= \frac{1}{\Delta}\begin{pmatrix}1 & f_m G_{ms} \\ f_s G_{sm} & 1\end{pmatrix}\begin{pmatrix}a_m \\ a_s\end{pmatrix}\end{aligned} \tag{10}$$

where we have introduced the (implicitly defined) *coupling coefficients* G_{ms} and G_{sm}, dimensionless quantities that quantify the nanoparticle-to-sphere coupling and which only depend on the relative orientations and separation distances between these objects and not on the frequencies.[35] In this equation, Δ is the determinant of the *coupling matrix* which for this simple case is given by $\Delta = 1 - f_m(\omega)\, f_s(\omega)\, G_{ms}G_{sm}$.

The scattering spectrum of this simple coupled system is proportional to $|\tilde{a}_i|^2 \propto 1/|\Delta|^2$,[36] meaning that the resonances of this coupled system occur for frequencies ω which satisfy $1 = f_m(\omega)\, f_s(\omega)\, G_{ms}G_{sm}$. In order to obtain closed analytical forms that predict the values of these frequencies, we employ the following approximate forms of $f(\omega)$ for both the single emitter and the metallic nanoparticle, which have been derived in the Supporting Information [eqs S11 and S12]:

dx.doi.org/10.1021/jp506402m | J. Phys. Chem. C 2014, 118, 23963−23969

$$f_s(\omega) \approx -\frac{f\omega_o/2}{\omega - \omega_o - \frac{f\omega_o}{6\varepsilon_b} + i\frac{\Gamma}{2}}$$

$$f_m(\omega) \approx -\frac{2\gamma_{pm}^2}{(\gamma_{pm}-1)^2}\frac{\omega_m^3}{\omega_P^2}\frac{\varepsilon_b^2}{\omega - \tilde{\omega}_m} \quad (11)$$

With these, the resonance condition leads to the following quadratic equation for the resonance frequencies of the coupled system:

$$(\omega - \tilde{\omega}_m)\left(\omega - \omega_o - \frac{f\omega_o}{6\varepsilon_b} + i\frac{\Gamma}{2}\right) = g_{pm}^2 \quad (12)$$

where we have defined the plasmon−exciton coupling constant as

$$g_{pm}^2 = \frac{2\gamma_{pm}^2}{(\gamma_{pm}-1)^2}\frac{\omega_m^3}{\omega_P^2} \times \frac{f\omega_o}{2} \times \varepsilon_b^2 G_{ms}G_{sm}$$

$$= g_P \times \frac{f\omega_o}{2} \times \varepsilon_b^2 G_{ms}G_{sm} \quad (13)$$

which we have conveniently written as a product of three factors: the first one depends on the properties of the metal nanoparticle(s) through the eigenvalue γ_{pm} (fixed by the shape and geometrical properties of the particle(s)), the resonance frequency of the plasmon mode ω_m which is fixed by both γ_{pm} and the dielectric constant of the surrounding medium (ε_b), and ω_P the bulk plasma frequency of the metal. The second term depends solely on the properties of the single emitter, namely the magnitude of its oscillator strength f and resonance frequency ω_o. The last term depends on the near-fields around the particle and emitter in addition to the their relative orientations. *Thus, unlike the case of a homogeneous and infinite coating around the metal nanoparticles, the magnitude of the coupling strength depends critically on the placement of this emitter in relation to the electric near-field produced by the localized surface plasmon resonance (implicit in $G_{ms}G_{sm}$).* Again, in this case, the strong coupling condition also reads (at resonance) $g_{pm}^2 > (\Gamma - \Gamma_m)^2/16$ in agreement with our previous derivation. This simple derivation can be easily extended to account for the case where the excitonic material is not uniformly distributed around the metal nanoparticle nor in the form of a single emitter but, instead, is distributed in a specific shape or "patch" with a dimension comparable to the nanoparticle. Under the assumption that this patch contains N nonmutually interacting dipoles, f is simply scaled by this number density, and trivially one substitutes f for Nf in the expression shown above for g_{pm}^2, bearing in mind that $\vec{E}_s$ represents the collective electric field produced by the patch acting on the metal nanoparticle. The resulting expression for g_{pm}^2 correctly predicts the scaling of the coupling strength with the number of oscillators (N) as calculated by more complex approaches.[45,46]

With these derivations, we can now address the important question as to how, in the most general instance, one could design a plasmon−exciton coupled system that exhibits strong coupling. To this end, we consider each of the three terms contributing to the coupling constant of eq 13. In Figure 4a we show how the plasmonic contribution evolves as a function of localized surface plasmon resonance frequency. The most salient feature of this graph is that, for both Au and Ag, the magnitude of this contribution is almost an order of magnitude

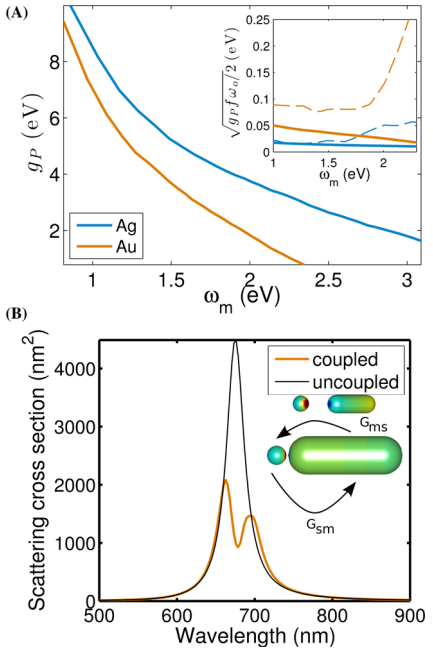

Figure 4. (A) Plasmonic contribution to the coupling constant of eq 13 plotted as a function of localized surface plasmon resonance ω_m in a medium with ε_b = 2.25. The inset shows the value of $(gP \times ((f\omega_o)/2))^{1/2}$. (B) Calculated scattering spectra of the isolated rod and the coupled system for ε_b =2.25, Au and assuming that the parameters of DPDC describe the dielectric sphere. Inset: Diagram of a coupled system consisting of a nanorod of 20 nm in diameter and 48 nm in length separated by 2 nm from a dielectric sphere of 5 nm radius. The colors indicate the relative surface charge densities. G_{sm} and G_{ms} are the geometrical coupling coefficients discussed in the text.

bigger than those obtained in Figure 2a. Furthermore, unlike the case shown in that figure, the plasmonic contribution to the coupling strength is predicted to increase with decreasing frequency of the localized surface plasmon resonance. The second contribution to g_{pm}^2 of eq 13 is simply $f\omega_o/2$, stating that excitonic materials with a high value of f are required for achieving strong coupling. In the inset of Figure 4a we show how the value of $[g_P \times ((f\omega_o)/2)]^{1/2}$ evolves vs the localized plasmon frequency for Au and Ag nanoparticles, along with the intrinsic plasmon line width (dashed lines) for the case of ω_o = 1.79 eV (like the DPDC J-aggregates[29]) but with $f = 4 \times 10^{-3}$ for the case of Au nanoparticles, whereas for Ag $f = 4 \times 10^{-4}$. These correspond to the minimum values for which $[g_P \times ((f\omega_o)/2)]^{1/2}$ remains above the intrinsic plasmon line width (dashed lines in inset of Figure 4a).

However, one also needs to account for the last term of eq 13, which involves the product of the geometrical coupling factors $\varepsilon_b^2 G_{ms}G_{sm}$.[35−37,41] In order to assess the order of magnitude of these geometrical coupling constants, one must evaluate these quantities for a specific case. As an example, we show in Figure 4b a single metal nanorod (diameter = 20 nm, length = 48 nm, dimensions chosen to represent a chemically synthesized Au nanorod) separated by 2 nm from a dielectric sphere of radius of 5 nm (size chosen to approximate a typical colloidal QD). The geometry is chosen in such a way that the dielectric sphere is positioned very close to the points of maximum electric near-field created by the longitudinal plasmon resonance of the rod, this with the aim of increasing the values of $G_{ms}G_{sm}$. For this configuration a numerical evaluation of the geometric coupling constants (using

dx.doi.org/10.1021/jp506402m | J. Phys. Chem. C 2014, 118, 23963−23969

Matlab[52]) yields $\varepsilon_b^2 G_{ms} G_{sm} \approx 0.19$, which implies a further decrease in the total value of the coupling constant shown in Figure 4a. Other configurations can lead to higher values (such as a nanorod dimer[51,53]).

The key results of this manuscript are the expressions for the plasmon−exciton coupling strengths given by eqs 7 and 13, each expressing the contributions of the plasmonic and excitonic material to their interactions in addition to factors that arise from the geometry of the coupling. Our approach is different from previous analytical studies of plasmon−exciton coupling,[53,54] which have relied on purely phenomenological models of (classical) coupled oscillators. In these phenomenological models, the magnitude of the coupling strength is introduced as a free parameter not explicitly connected to the plasmonic, excitonic, or geometrical properties of the coupled system.

Our formalism is limited to those plasmon-supporting structures that are sub-wavelength sized where implicitly retardation effects are not included.[55] Furthermore, all the derivations that led to these results are semiclassical: the electromagnetic fields were solely described by using Maxwell's equations (no field quantization) whereas the quantum mechanical nature of the electronic transitions in the active medium are taken into account implicitly in the expressions for the permittivities of the excitonic materials. Only properties beyond a semiclassical approach, such as photon statistics or higher order correlations, require a quantum mechanical treatment (such as the one presented by Manjavacas et al.[56]).

Our results make a number of key predictions which are very important for designing strongly coupled plasmon−exciton systems. In particular, we have found, for the case when the excitonic material uniformly covers the plasmon supporting structures, the following: (i) strong coupling occurs when the plasmonic and excitonic elements resonate in the spectral region between 1.5 to 2 eV (Figure 2a); (ii) the coupling strength is highest when the excitonic transition frequency is slightly higher than that of the uncoupled localized surface plasmon resonance; and (iii) strong coupling can only be achieved for excitonic materials with reduced oscillators strengths f (eq 2) larger than 4×10^{-3}.

■ ASSOCIATED CONTENT

Supporting Information

Detailed information on some derivations as mentioned in the text. This material is available free of charge via the Internet at http://pubs.acs.org.

■ AUTHOR INFORMATION

Corresponding Author

*E-mail: daniel.gomez@csiro.au.

Notes

The authors declare no competing financial interest.

■ ACKNOWLEDGMENTS

D.E.G. and T.J.D. acknowledge support through a guest professorship from MPI FKF. This work was performed in part at the Melbourne Centre for Nanofabrication (MCN) in the Victorian Node of the Australian National Fabrication Facility (ANFF). D.E.G. would like to thank the ARC for support through a Discovery Project DP110101767. D.E.G. and T.J.D. acknowledge the ANFF for the MCN Technology Fellowships. H.G. would like to thank DFG, BMBF, Baden-Württemberg Stiftung and ERC (complex plasmonics), Zeiss-Stiftung and an ERC Advanced Grant (COMPLEXPLAS).

■ REFERENCES

(1) Fofang, N. T.; Park, T.-H.; Neumann, O.; Mirin, N. A.; Nordlander, P.; Halas, N. J. Plexcitonic Nanoparticles: Plasmon-Exciton Coupling In Nanoshell-J-Aggregate Complexes. *Nano Lett.* **2008**, *8*, 3481−3487.

(2) Bellessa, J.; Bonnand, C.; Plenet, J. C.; Mugnier, J. Strong Coupling between Surface Plasmons and Excitons in an Organic Semiconductor. *Phys. Rev. Lett.* **2004**, *93*, 036404.

(3) Dintinger, J.; Klein, S.; Bustos, F.; Barnes, W. L.; Ebbesen, T. W. Strong Coupling between Surface Plasmon-Polaritons and Organic Molecules in Subwavelength Hole Arrays. *Phys. Rev. B* **2005**, *71*, 035424.

(4) Bonnand, C.; Bellessa, J.; Plenet, J. C. Properties of Surface Plasmons Strongly Coupled to Excitons in an Organic Semiconductor near a Metallic Surface. *Phys. Rev. B* **2006**, *73*, 245330.

(5) Bonnand, C.; Bellessa, J.; Symonds, C.; Plenet, J. C. Polaritonic Emission via Surface Plasmon Cross Coupling. *Appl. Phys. Lett.* **2006**, *89*, 231119.

(6) Dintinger, J.; Klein, S.; Ebbesen, T. W. Molecule-Surface Plasmon Interactions in Hole Arrays: Enhanced Absorption, Refractive Index Changes, and All-Optical Switching. *Adv. Mater.* **2006**, *18*, 1267−1270.

(7) Dintinger, J.; Robel, I.; Kamat, P.; Genet, C.; Ebbesen, T. Terahertz All-Optical Molecule-Plasmon Modulation. *Adv. Mater.* **2006**, *18*, 1645−1648.

(8) Sugawara, Y.; Kelf, T. A.; Baumberg, J. J.; Abdelsalam, M. E.; Bartlett, P. N. Strong Coupling between Localized Plasmons and Organic Excitons in Metal Nanovoids. *Phys. Rev. Lett.* **2006**, *97*, 266808.

(9) Symonds, C.; Bellessa, J.; Plenet, J. C.; Bréhier, A.; Parashkov, R.; Lauret, J. S.; Deleporte, E. Emission of Hybrid Organic-Inorganic Exciton/Plasmon Mixed States. *Appl. Phys. Lett.* **2007**, *90*, 091107.

(10) Wurtz, G.; Evans, P.; Hendren, W.; Atkinson, R.; Dickson, W.; Pollard, R.; Zayats, A.; Harrison, W.; Bower, C. Molecular Plasmonics with Tunable Exciton- Plasmon Coupling Strength in J-Aggregate Hybridized Au Nanorod Assemblies. *Nano Lett.* **2007**, *7*, 1297−1303.

(11) Bellessa, J.; Symonds, C.; Meynaud, C.; Plenet, J. C.; Cambril, E.; Miard, A.; Ferlazzo, L.; Lemaître, A. Exciton/Plasmon Polaritons in $GaAs/Al_{0.93}Ga_{0.07}As$ Heterostructures Near a Metallic Layer. *Phys. Rev. B* **2008**, *78*, 205326.

(12) Symonds, C.; Bonnand, C.; Plenet, J. C.; Brehier, A.; Parashkov, R.; Lauret, J. S.; Deleporte, E.; Bellessa, J. Particularities of Surface Plasmon-Exciton Strong Coupling with Large Rabi Splitting. *New J. Phys.* **2008**, *10*, 065017 (11 pp).

(13) Vasa, P.; Pomraenke, R.; Schwieger, S.; Mazur, Y. I.; Kunets, V.; Srinivasan, P.; Johnson, E.; Kihm, J. E.; Kim, D. S.; Runge, E.; Salamo, G.; Lienau, C. Coherent Exciton-Surface-Plasmon-Polariton Interaction in Hybrid Metal-Semiconductor Nanostructures. *Phys. Rev. Lett.* **2008**, *101*, 116801.

(14) Hakala, T. K.; Toppari, J. J.; Kuzyk, A.; Pettersson, M.; Tikkanen, H.; Kunttu, H.; Törmä, P. Vacuum Rabi Splitting and Strong-Coupling Dynamics for Surface-Plasmon Polaritons and Rhodamine 6G Molecules. *Phys. Rev. Lett.* **2009**, *103*, 053602.

(15) Salomon, A.; Genet, C.; Ebbesen, T. Molecule-Light Complex: Dynamics of Hybrid Molecule-Surface Plasmon States. *Angew. Chem., Int. Ed.* **2009**, *48*, 8748−8751.

(16) Yoshida, A.; Uchida, N.; Kometani, N. Synthesis and Spectroscopic Studies of Composite Gold Nanorods with a Double-Shell Structure Composed of Spacer and Cyanine Dye J-Aggregate Layers. *Langmuir* **2009**, *25*, 11802−11807.

(17) Yoshida, A.; Yonezawa, Y.; Kometani, N. Tuning of the Spectroscopic Properties of Composite Nanoparticles by the Insertion of a Spacer Layer: Effect of Exciton−Plasmon Coupling. *Langmuir* **2009**, *25*, 6683−6689.

(18) Gómez, D. E.; Vernon, K. C.; Mulvaney, P.; Davis, T. J. Surface Plasmon Mediated Strong Exciton-Photon Coupling in Semiconductor Nanocrystals. *Nano Lett.* **2010**, *10*, 274−278.

(19) Gómez, D. E.; Vernon, K. C.; Mulvaney, P.; Davis, T. J. Coherent Superposition Of Exciton States In Quantum Dots Induced by Surface Plasmons. *Appl. Phys. Lett.* **2010**, *96*, 073108.
(20) Ni, W.; Ambjornsson, T.; Apell, S. P.; Chen, H.; Wang, J. Observing Plasmonic-Molecular Resonance Coupling on Single Gold Nanorods. *Nano Lett.* **2010**, *10*, 77−84.
(21) Vasa, P.; Pomraenke, R.; Cirmi, G.; De Re, E.; Wang, W.; Schwieger, S.; Leipold, D.; Runge, E.; Cerullo, G.; Lienau, C. Ultrafast Manipulation of Strong Coupling in Metal-Molecular Aggregate Hybrid Nanostructures. *ACS Nano* **2010**, *4*, 7559−7565.
(22) Berrier, A.; Cools, R.; Arnold, C.; Offermans, P.; Crego-Calama, M.; Brongersma, S. H.; Gómez-Rivas, J. Active Control of the Strong Coupling Regime between Porphyrin Excitons and Surface Plasmon Polaritons. *ACS Nano* **2011**, *5*, 6226.
(23) Fofang, N. T.; Grady, N. K.; Fan, Z.; Govorov, A. O.; Halas, N. J. Plexciton Dynamics: Exciton-Plasmon Coupling in a J-Aggregate-Au Nanoshell Complex Provides a Mechanism for Nonlinearity. *Nano Lett.* **2011**, *11*, 1556−1560.
(24) Hao, Y.-W.; Wang, H.-Y.; Jiang, Y.; Chen, Q.-D.; Ueno, K.; Wang, W.-Q.; Misawa, H.; Sun, H.-B. Hybrid-State Dynamics Of Gold Nanorods/Dye J-Aggregates under Strong Coupling. *Angew. Chem., Int. Ed.* **2011**, *50*, 7824−8.
(25) Schwartz, T.; Hutchison, J. A.; Genet, C.; Ebbesen, T. W. Reversible Switching of Ultrastrong Light-Molecule Coupling. *Phys. Rev. Lett.* **2011**, *106*, 196405.
(26) Aberra Guebrou, S.; Symonds, C.; Homeyer, E.; Plenet, J. C.; Gartstein, Y. N.; Agranovich, V. M.; Bellessa, J. Coherent Emission from a Disordered Organic Semiconductor Induced by Strong Coupling with Surface Plasmons. *Phys. Rev. Lett.* **2012**, *108*, 066401.
(27) Rodriguez, S. R. K.; Verschuuren, M. A.; Rivas, J. G. Bose−Einstein Condensation Of Plexcitons; **2012**; arXiv:1210.7086.
(28) Gomez, D.; Lo, S. S.; Davis, T. J.; Hartland, G. V. Pico-Second Kinetics of Strongly Coupled Excitons and Surface Plasmon Polaritons. *J. Phys. Chem. B* **2013**, *117*, 4340−4346.
(29) Schlather, A. E.; Large, N.; Urban, A. S.; Nordlander, P.; Halas, N. J. Near-Field Mediated Plexcitonic Coupling and Giant Rabi Splitting in Individual Metallic Dimers. *Nano Lett.* **2013**, *13*, 3281.
(30) Vasa, P.; Wang, W.; Pomraenke, R.; Lammers, M.; Maiuri, M.; Manzoni, C.; Cerullo, G.; Lienau, C. Real-Time Observation Of Ultrafast Rabi Oscillations Between Excitons and Plasmons in Metal Nanostructures With J-Aggregates. *Nat. Photon* **2013**, *7*, 128−132.
(31) Zengin, G.; Johansson, G.; Johansson, P.; Antosiewicz, T. J.; Kall, M.; Shegai, T. Approaching The Strong Coupling Limit in Single Plasmonic Nanorods Interacting with J-Aggregates. *Sci. Rep.* **2013**, *3*.
(32) Kena-Cohen, S.; Forrest, S. R. Room-Temperature Polariton Lasing in an Organic Single-Crystal Microcavity. *Nat. Photon* **2010**, *4*, 371−375.
(33) Deng, H.; Weihs, G.; Snoke, D.; Bloch, J.; Yamamoto, Y. Polariton Lasing vs Photon Lasing in a Semiconductor Microcavity. *Proc. Natl. Acad. Sci. U.S.A.* **2003**, *100*, 15318−15323.
(34) Gomez, D. E.; Davis, T. J.; Funston, A. M. Plasmonics by Design: Design Principles to Structure-Function Relationships with Assemblies of Metal Nanoparticles. *J. Mater. Chem. C* **2014**, *2*, 3077−3087.
(35) Davis, T. J.; Gómez, D. E.; Vernon, K. C. Simple Model for the Hybridization of Surface Plasmon Resonances in Metallic Nanoparticles. *Nano Lett.* **2010**, *10*, 2618−2625.
(36) Davis, T. J.; Vernon, K. C.; Gómez, D. E. Designing Plasmonic Systems Using Optical Coupling between Nanoparticles. *Phys. Rev. B* **2009**, *79*, 155423.
(37) Gómez, D. E.; Vernon, K. C.; Davis, T. J. Symmetry Effects On The Optical Coupling between Plasmonic Nanoparticles with Applications to Hierarchical Structures. *Phys. Rev. B* **2010**, *81*, 075414.
(38) Vernon, K. C.; Funston, A. M.; Novo, C.; Gómez, D. E.; Mulvaney, P.; Davis, T. J. Influence of Particle-Substrate Interaction on Localized Plasmon Resonances. *Nano Lett.* **2010**, *10*, 2080−2086.
(39) Funston, A. M.; Gómez, D. E.; Karg, M.; Vernon, K. C.; Davis, T. J.; Mulvaney, P. Aligned Linear Arrays of Crystalline Nanoparticles. *J. Phys. Chem. Lett.* **2013**, *4*, 1994−2001.
(40) Barrow, S. J.; Funston, A. M.; Gómez, D. E.; Davis, T. J.; Mulvaney, P. Surface Plasmon Resonances in Strongly Coupled Gold Nanosphere Chains from Monomer to Hexamer. *Nano Lett.* **2011**, *11*, 4180−4187.
(41) Davis, T. J.; Hentschel, M.; Liu, N.; Giessen, H. Analytical Model of the Three-Dimensional Plasmonic Ruler. *ACS Nano* **2012**, *6*, 1291−1298.
(42) Davis, T. J.; Hendry, E. Superchiral Electromagnetic Fields Created By Surface Plasmons In Nonchiral Metallic Nanostructures. *Phys. Rev. B* **2013**, *87*, 085405.
(43) Eftekhari, F.; Davis, T. J. Strong Chiral Optical Response From Planar Arrays Of Subwavelength Metallic Structures Supporting Surface Plasmon Resonances. *Phys. Rev. B* **2012**, *86*, 075428.
(44) Gómez, D. E.; Teo, Z.-Q.; Altissimo, M.; Davis, T.; Earl, S.; Roberts, A. The Dark Side Of Plasmonics. *Nano Lett.* **2013**, *13*, 3722−3728.
(45) Andreani, L. C.; Panzarini, G.; Gérard, J.-M. Strong-Coupling Regime for Quantum Boxes in Pillar Microcavities: Theory. *Phys. Rev. B* **1999**, *60*, 13276−13279.
(46) Rudin, S.; Reinecke, T. L. Oscillator Model For Vacuum Rabi Splitting In Microcavities. *Phys. Rev. B* **1999**, *59*, 10227−10233.
(47) Reithmaier, J. P.; Sek, G.; Loffler, A.; Hofmann, C.; Kuhn, S.; Reitzenstein, S.; Keldysh, L. V.; Kulakovskii, V. D.; Reinecke, T. L.; Forchel, A. Strong Coupling in a Single Quantum Dot-Semiconductor Microcavity System. *Nature* **2004**, *432*, 197−200.
(48) Novo, C.; Gomez, D.; Perez-Juste, J.; Zhang, Z.; Petrova, H.; Reismann, M.; Mulvaney, P.; Hartland, G. V. Contributions from Radiation Damping and Surface Scattering to the Linewidth of the Longitudinal Plasmon Band of Gold Nanorods: A Single Particle Study. *Phys. Chem. Chem. Phys.* **2006**, *8*, 3540−3546.
(49) Sönnichsen, C.; Franzl, T.; Wilk, T.; von Plessen, G.; Feldmann, J.; Wilson, O.; Mulvaney, P. Drastic Reduction of Plasmon Damping in Gold Nanorods. *Phys. Rev. Lett.* **2002**, *88*, 077402.
(50) Davis, T. J.; Gómez, D. E.; Vernon, K. C. Interaction of Molecules with Localized Surface Plasmons in Metallic Nanoparticles. *Phys. Rev. B* **2010**, *81*, 045432.
(51) Gómez, D. E.; Roberts, A.; Davis, T. J.; Vernon, K. C. Surface Plasmon Hybridization And Exciton Coupling. *Phys. Rev. B* **2012**, *86*, 035411.
(52) Hohenester, U.; Trugler, A. MNPBEM a Matlab Toolbox for the Simulation of Plasmonic Nanoparticles. *Comput. Phys. Commun.* **2012**, *183*, 370−381.
(53) Wu, X.; Gray, S. K.; Pelton, M. Quantum-Dot-Induced Transparency in a Nanoscale Plasmonic Resonator. *Opt. Express* **2010**, *18*, 23633−23645.
(54) Faucheaux, J. A.; Fu, J.; Jain, P. K. Unified Theoretical Framework for Realizing Diverse Regimes of Strong Coupling between Plasmons and Electronic Transitions. *J. Phys. Chem. C* **2014**, *118*, 2710−2717.
(55) Antosiewicz, T. J.; Apell, S. P.; Shegai, T. Plasmon-Exciton Interactions in a Core-Shell Geometry: From Enhanced Absorption to Strong Coupling. *ACS Photonics* **2014**, *1*, 454−463.
(56) Manjavacas, A.; Abajo, F. J. G. d.; Nordlander, P. Quantum Plexcitonics: Strongly Interacting Plasmons and Excitons. *Nano Lett.* **2011**, *11*, 2318−2323.